DYNAMIC TENSILE EXPERIMENTS OF HARD RUBBER ON INSTRON TEST MACHINE UNDER FINITE DEFORMATIONS

Šulc P., Pešek L., Bula V., Šnábl P. [*]

Abstract: *This paper deals with the first experimental tests of hard rubbers under tensile harmonic loading on the axial-torsional servohydraulic Instron 8852 test machine. The objective of these experiments on cylindrical rubber specimens on this machine is to obtain stress-strain curves of rubber specimens, first considering uniaxial finite longitudinal strains for a single load cycle. Next, the hysteresis loops and their skeleton curves are compared for two selected strain measures as a function of their conjugate stress. It is shown how to obtain the dependence between elongation in the axial direction and constriction in the radial direction, which is used to determine the Cauchy stress in this configuration.*

Keywords: Uniaxial harmonic loading, finite deformation, Green-Lagrange strain tensor, second Piola-Kirchhoff stress, hysteresis loop.

1. Introduction

Unlike the conventional structural materials, rubber materials under dynamic loading exhibit a nonlinear time-varying behavior due to the strain, viscosity, and temperature dependences (Pešek, 2008). In our laboratory, we have been testing hard rubbers for passive vibration damper applications (Šulc, 2016). Based on the experiments we focus on identification of material characteristics of hard synthetic rubbers with Sh>60 such as loss factor, damping and modulus of elasticity in dependence on temperature, strain and frequency loadings (Šulc,2017).

Since rubber dampers in many cases work at quasi-harmonic, low frequency and large deformations, e.g. silent blocks of heavy machinery, we have recently been working on finding a simple model of hard rubber damping applicable to large deformations. Therefore, an experimental apparatus for torsional dynamic loading of rubber specimens (Korobeynikov, 2022) of circular cross-section was first designed and built to determine the thermal-viscous-elastic properties of the material at small and finite strains, different amplitudes, frequencies and temperatures. A simple damping model called the hyperelastic proportional damping (HPD) model was proposed to account for large deformations to facilitate structural calculations (Šulc, 2021). Since we consider finite strain under load, we rely on the principles of hyperelasticity (Korobeynikov, 2022, Liu, 2022) to obtain the strain energy.

In this paper, we discuss the first experimental results obtained on an Instron 8852 servohydraulic machine under harmonic tensile loading. A cylindrical EPDM rubber material specimen with a Shore 80 hardness was tested on this machine. The measured outputs of this machine are the loading forces and strain magnitude under harmonic tensile loading considering large strains (25%). From these experimental outputs, stress-strain curves are evaluated as a function of selected conjugate quantities. Furthermore, the determination of the transverse constriction of the specimen for different strain magnitudes is described.

[*] Ing. Petr Šulc, PhD., Ing. Luděk Pešek, CSc., Ing. Vitězslav Bula, Ing. Pavel Šnábl: Institute of Thermomechanics of the CAS, v. v. i.,Dolejškova 1402/5, 182 00 Prague; CZ, sulc@it.cas.cz

2. Description of experimental rubber testing

The dynamic tensile tests were measured on an Instron 8852 testing machine. On this machine, a rubber cylindrical specimen made of EPDM materials with dimensions of 0.03 m diameter and 0.1 m length with glued metal surfaces with pins for attachment to the clamping head was tested. These measurements were performed at ambient temperature (22 °C) with excitation frequencies ranging from 1 Hz to 5 Hz for different strain amplitudes, up to a magnitude of 25% strain. The tests were carried out for the following loading modes, namely alternating (symmetrical and asymmetrical) or repeated loading. The control of these experiments was by force control or by deflection. Control by deflection was the best way to obtain only tensile strain. During testing only nine load cycles for each frequency were performed. The reason of a few loading cycles is that the rubber could change its stiffness with longer time and thus the response amplitudes to increase. For each amplitude and frequency, five loading cycles were selected to express the hysteresis loop and its skeleton curve. The dissipated energy and skeleton curve are subsequently evaluated from the hysteresis loop. Skeleton curves are used to tune the strain energy density constants of appropriate hyperelastic models. Under tensile loading, the large deformations cause biaxial deformation in the longitudinal and transverse directions. Therefore, we focused on determination of the dependence of the longitudinal on the transverse (radial) deformation. For this purpose, a static load was applied to stretch the specimen by increment 0.005 m up to the maximum deformation 40% of the specimen elongation. After each of these static deformations, the diameters of the deformed rubber specimen were measured at three locations.

3. Experimental results

The example of experimental outputs, i.e. excitation force F and its response y versus time for two excitation frequencies 2 Hz and 4 Hz with amplitude 0.025m corresponding to 25% strain of the sample, can be seen in Fig.1.
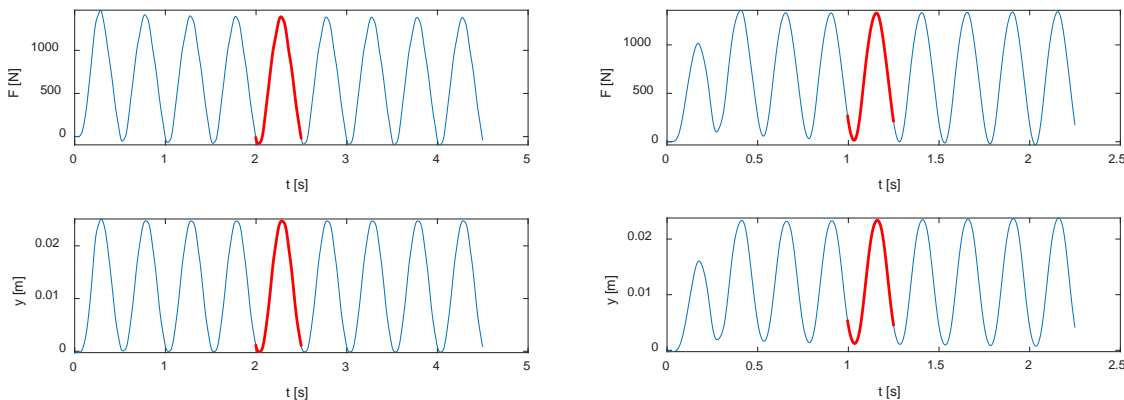

Fig. 1: Dependence of harmonic force F and displacement y on time for excitation frequencies 2Hz (left) and 4Hz (right).

To plot the hysteresis loops, the Green-Lagrange strain and Cauchy strain were chosen. Therefore, it was necessary to use appropriate stress measures to suit the selected strain measures so that their scalar product would match the work. For uniaxial tension, the second Piola-Kirchoff stress S and the Cauchy "true" stress T, respectively, as the conjugate stress measures to chosen strains can be expressed

$$S_{11} = \frac{P_t l_0}{A_0 l_t}; \quad T_{11} = \frac{P_t}{A_t}, \tag{1}$$

where P_t is the amplitude of harmonic force, l_t is the length of the specimen after deformation, l_0 is the initial length, A_t is the area after deformation and A_0 is the area before deformation. To determine the Cauchy "true" stress T, it was necessary to determine the size of the actual area A_t of the stretched rubber specimen. A static stretching of the specimen was used to determine this area in order to determine its

narrowed diameter D_i. The specimen was loaded with a static tensile force in successive steps to achieve a deformation of 0.005 m at each step up to a maximum deformation of 0.04 m. In these incremental steps, the individual diameters D_i of the specimen and the static forces F_i inducing these individual static deformations were recorded. Measurements of the specimen diameter D_i were taken at three locations on the specimen, namely at the centre and at a distance of 0.01 m from the bonded metal surfaces. In each of these nine deformed regions of sample, a linear relationship was used to determine the magnitude of the deformed diameters D_i, which is as follows

$$D_j = D_{(i-1)stat} + \left(y_j - y_{(i-1)stat} \right) \cdot \left(\frac{D_{(i-1)stat} - D_{(i)stat}}{y_{(i-1)stat} - y_{(i)stat}} \right), i = 1, \ldots, k, j = 1 \ldots, l, , \tag{2}$$

where D_j is the searched diameter, y_j is the obtained deflection from the harmonic tensile load, index j is the number of samples per period of harmonic load, $y_{(i)stat}$ is the given static deformation, $D_{(i)stat}$ is the size of the diameter corresponding to the given static deformation $y_{(i)stat}$ of the specimen.

Figure 2 shows the hysteresis loops as a function of four amplitudes, i.e. 0.01 m (black); 0.015 m (blue); 0.02 m (green); 0.025 m (red), with repeated tensile loads with an excitation frequency of 4 Hz. The hysteresis loops for the conjugate measures of the Cauchy "true" stress and the Cauchy strain are shown in the left figure, and the hysteresis loops for the conjugate measures of the second Piola-Kirchoff stress and the Green-Lagrange strain are shown in the right figure. The difference between the hysteresis curves can be seen, where the hysteresis loop on the right leans more towards the general stress-strain curve of hard rubber materials with increasing strain.
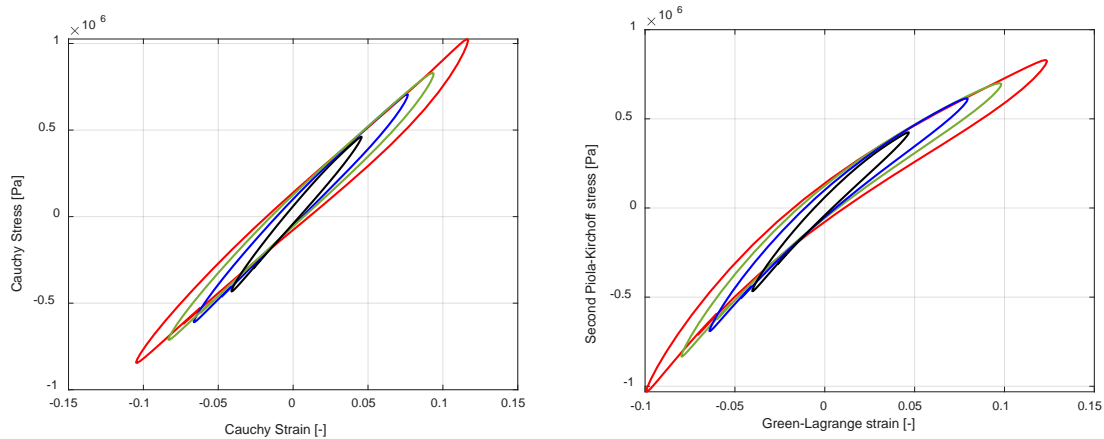

Fig. 2: Comparison of the hysteresis curves as a function of the magnitude of the loading amplitudes: Cauchy "true" stress vs Cauchy strain (left), second Piola-Kirchoff stress vs Green-Lagrange strain (right).

The experimental skeleton curves used to enumerate the strain energy of the hyperelastic models were evaluated as mean lines from experimental hysteresis loops for each excitation amplitude. Comparison for the two types of skeleton curves, i.e. Cauchy stress vs Cauchy strain (red) and the second Piola-Kirchoff stress vs Green-Lagrange strain (blue), is shown in Fig. 3 left. Figure 3 right shows the hysteresis curves for both previous cases (keeping color designation) for different excitation frequencies (from 1Hz to 5Hz) at the same amplitude 0.025m. This graph shows the minimal dependence of these curves on the excitation frequency.
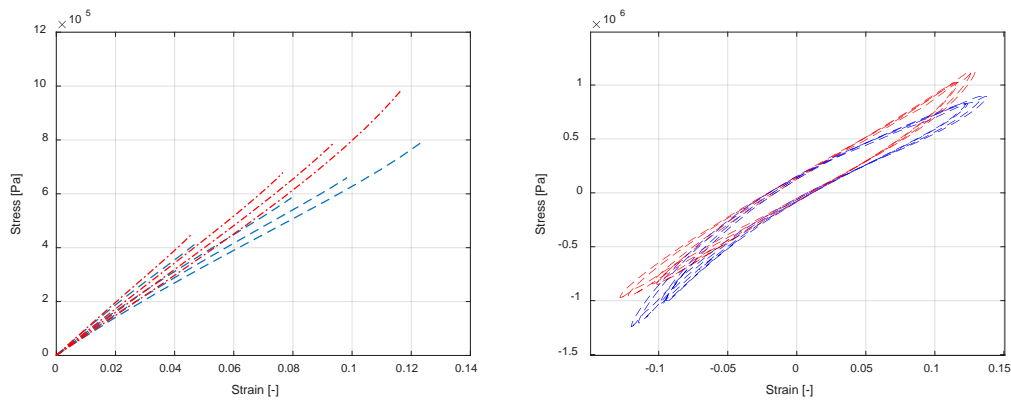
Fig. 3: Experimental skeleton curves (left) and hysteresis loops for different frequencies (right).

3. Conclusions

This paper deals with experimental tests of hard rubbers under dynamic tensile loading. The results presented in this paper are used to obtain the dissipated and deformed energy for different amplitudes and frequencies under harmonic tensile loading. The obtained results will be used to verify the proposed HPD damping model of hard rubbers (Šulc, 2021). Furthermore, the procedure was proposed to obtain the Cauchy "true" stress based on the sample diameter measurements, which will be further refined by using line scanner sensor or camera snapshots. The dynamic tests of these rubber samples will be performed on the newly developed tensile test rig in our laboratory and the achieved results will be used to validate this new test rig.

Acknowledgement

References

Korobeynikov, S.N., Larichkin, A.Yu. and Rotanova, T.A. (2022) Hyperelasticity models extending Hooke's law from small to moderate strainsand experimental verification of their scope of application. International Journal of Solids and Structures, 252, p. .

Korobeynikov, S..N., Larichkin, A.Yu. and Rotanova, T.A. (2022) Simulating cylinder torsion using Hill's linear isotropic hyperelastic material models. Mechanics of Time-Dependent Materials, p. 1-31.

Liu, C-H., Hung P-T. (2022) Effect of the Infill Density on the Performance of a 3D-Printed Compliant Finger. Materials & Design, 223.

Pešek, L., Půst, L., Balda, M., Vaněk, F., Svoboda, J., Procházka, P., Marvalová, B.(2008) Investigation of dynamics and reliability of rubber segments for resilent wheel, Procs. of ISMA 2008, KU Leuven,pp. 2887-2902.

Šulc, P., Kopačka, J., Pešek, L., Bula, V. (2021). Hyperelastic proportional damping for numerical non-conservative dynamic models of hard rubbers under large deformations, Int. J. Non. Linear. Mech., Roč. 137, s. 103823.

Šulc, P., Pešek, L., Bula, V., Cibulka, J. Boháč, T., Tašek, H. (2017) Pre-stressed rubber material constant estimation for resilient wheel application. Advances in Engineering Software, 113, p.p. 76-83.

Šulc P., Pešek L., Bula V., Cibulka J., Košina J. (2017) Proposal of hyperelastic proportional damping as dissipated energy model of hard rubbers, Eng. Mech., p. p. 15–18.

Šulc P., Pešek L., Bula V., Cibulka J., Košina J. (2016) Amplitude-temperature analysis of hard rubber by torsional vibration. Journal of Applied Mechanics and Materials. Roč. 821, p p.. 295-302.